

PACS numbers: 42.65.An; 42.65.Dr; 42.60.Jf
DOI: 10.1070/QE2009v039n07ABEH014019

Stimulated Raman scattering spectrum of Gaussian and Bessel light beams

P.A. Apanasevich, R.V. Chulkov, A.S. Grabtchikov, V.A. Orlovich, G.I. Timofeeva

***Abstract*. The effect of the real part of the Raman susceptibility on the Stokes spectrum excited by Gaussian and Bessel beams is studied theoretically and experimentally. This part of the susceptibility is shown to be responsible for the increase in the overlap integral of the Stokes beam and the pump beam and, as a result, for the increase in the Raman amplification in the region of frequencies higher than the frequency of the exact Raman resonance. This, in particular, is observed in the spectral shift of the axial component of Raman generation in the case of Bessel pump and Stokes radiation in the case of the Gaussian pump to the high-frequency region. It is shown that the shift caused by the Bessel pump significantly exceeds the shift caused by the Gaussian pump. The conical component in the case of the Bessel pump is generated at the frequency of the exact Raman resonance.**

Keywords: *stimulated Raman scattering, Gaussian beam, Bessel beam, axicon.*

1. Introduction

Quasi-steady-state stimulated Raman scattering (SRS) is known to be described by the Raman susceptibility, which is a complex value proportional to the pump beam intensity and strongly dependent on the frequency of the scattered (Stokes) radiation. The imaginary part of this quantity is manifested in the Stokes radiation amplification (transfer of photons from the pump beam to the Stokes beam), while the real part leads to the change in the refractive index of the scattering medium at the Stokes frequency: to its increase in the region of frequencies higher than the frequency of the maximum of the imaginary part of the Raman susceptibility (exact Raman resonance) and to a decrease in the region of lower frequencies. Because of this, in the case of scattering of the spatially nonuniform pump the high-frequency and low-frequency components of the Stokes beam focus and defocus, respectively, which undoubtedly should lead to the frequency-dependent change in the spatial overlap of interacting fields, and, hence to the frequency dependence of the Raman amplification efficiency.

The fact, that the Raman susceptibility is a complex quantity, is known virtually from the first works on the Raman research [1, 2]. However, in most papers devoted to the Raman, the real part of this susceptibility, as a rule, is not taken into account. Obviously, the author of [3] was the first to observe experimentally the Stokes beam focusing resulting from the real part of the Raman susceptibility during the Raman amplification of the beam. The emergence of this part of the Raman susceptibility in the spectrum of the Raman amplification was considered later in papers [4, 5]. These papers showed theoretically and experimentally that in the case of the Gaussian pump the real part of the Raman susceptibility leads to a weak shift of the Raman gain maximum to the high-frequency range with respect to the frequency of the exact Raman resonance.

This paper is devoted to the theoretical and experimental investigation of the manifestation of the real part of the Raman susceptibility (or, in other words, the imaginary part of the Raman gain factor) in the spectrum of Raman generation in the case of pumping be the Bessel or Gaussian beams. It is shown that in the case of the Bessel pump the conical component of the Stokes beam is generated at the frequency of the exact Raman resonance and the axial component is significantly (up to $0.6\Delta v$, where Δv is the half-width of the spontaneous Raman line) shifted from it to the high-frequency region and that this shift of the axial component in the case of the Bessel pump significantly exceeds the spectral shift of the Stokes beam in the case of the Gaussian pump. The results of these studies were partially reflected in papers [6 – 8].

2. Theory

2.1 General relations

Let the SRS be excited by a highly monochromatic axially symmetric radiation beam. The scattered radiation beam even then should be axially symmetric with respect to the pump beam axis (the z axis) and its field $E(z,\rho)$ in the paraxial approximation can be found from the expression

$$\frac{\partial E(z,\rho)}{\partial z} = \left[\frac{\mathrm{i}}{2k}\,\Delta_\perp + \frac{1}{2}\,G_\delta S_\mathrm{p}(z,\rho)\right]E(z,\rho) + \sigma_\delta E_\mathrm{p}(z,\rho), \quad (1)$$

in which $E_\mathrm{p}(z,\rho)$ and $S_\mathrm{p}(z,\rho) = (cn_\mathrm{p}/2\pi)|E_\mathrm{p}(z,\rho)|^2$ are the amplitude and the intensity of the pump field; n_p is the is

P.A. Apanasevich, R.V. Chulkov, A.S. Grabtchikov, V.A. Orlovich, G.I. Timofeeva B.I. Stepanov Institute of Physics, National Academy of Sciences of Belarus, prosp. Nezavisimosti 68, 220072 Minsk, Belarus; e-mail: r.chulkov@dragon.bas-net.by, asg@dragon.bas-net.by

Received 8 December 2008
Kvantovaya Elektronika **39** (7) 615 – 623 (2009)
Translated by I.A. Ulitkin

the refractive index of the medium at the pump frequency ω_p; k is the wave number of scattered radiation; ρ is the transverse coordinate; $\Delta_\perp = \partial^2/\partial\rho^2 + (1/\rho)\partial/\partial\rho$ is the Laplacian in the plane of the beam cross section; σ_δ is the inverse length of spontaneous Raman scattering. The Raman susceptibility is taken into account in (1) by the complex value $G_\delta = G'_\delta + iG''_\delta$, where G'_δ is the Raman gain factor for the Stokes radiation determined by the real part of the Raman susceptibility and G''_δ is the parameter determined by its real part. In the case of the Lorentzian transition contour at which scattering occurs, we have $G_\delta = G_0(1 + i\delta)/(1 + \delta^2)$, where $\delta = (\omega - \omega_p + \Omega)T_2$ is the deviation of the frequency ω of scattered radiation from the frequency $\omega_p - \Omega$ corresponding to the exact Raman resonance; Ω and T_2 is the frequency andthe dephasing time of the vibration at which Raman scattering occurs. The last term in the right-hand side of (1) takes into account the spontaneous Raman scattering. Its spectral composition is determined by the relation $|\sigma_\delta|^2 \sim G'_\delta$.

In the case of weak scattering, the field $E_p(z, \rho)$ can be assumed to be the given function of the coordinates. Due to the linearity of equation (1) with respect to $E(z, \rho)$, the fields with different frequencies can be assumed independent.

Of practical interest is not the field $E(z, \rho)$ but the power $P_\delta(L) = cn\int_0^\infty |E(L, \rho)|^2 \rho d\rho$ of the scattered beam at the exit from the scattering medium of thickness L in the solid angle $\Delta\Phi$ and the frequency interval $\Delta\omega$, which are determined by the aperture and the spectral resolving power of the measuring device. To determine this quantity, equations

$$\frac{dP_\delta(z)}{dz} = G'_\delta S_p(z) M_\delta(z) P(z) + \eta G'_\delta P_\delta(z) \quad (2)$$

are easily derived from (1) [9], where $\eta = [\hbar\omega^3 n^2 \Delta\omega \times (\pi^2 c^2)^{-1}](\Delta\Phi/4\pi)$; $\hbar$ is the Planck constant; n is the refractive index;

$$M_\delta(z) = \int_0^\infty |F_p(z, \rho)|^2 |F(z, \rho)|^2 \rho d\rho \Big/ \int_0^\infty |F_p(z, \rho)|^2 \rho d\rho \quad (3)$$

is the normalised overlap integral of cross sections of the pump beam $[S_p(z, \rho) = S_p(z, 0)|F_p(z, \rho)|^2]$ and the Stokes beam $[E(z, \rho) = E(z, 0)\, F(z, \rho)]$. The expression for the coefficient η was found from the relation of the probabilities of the spontaneous and stimulated Raman transitions. This means that while deriving equation (2) we performed averaging in realisations of spontaneous scattering.

By assuming that z is measured from the input surface of the scattering medium, the general solution of equation (2) can be written in the form

$$P_\delta(z) = \left[P_\delta(0) + \eta G'_\delta \int_0^z P_p(z') \exp[-D_\delta(z')] dz'\right] \exp[D_\delta(z)], \quad (4)$$

where

$$D_\delta(z) = G'_\delta \int_0^z M_\delta(z') S_p(z') dz' \quad (5)$$

is the Raman gain. Its frequency dependence, as is seen from (5), is determined by the product of the Raman gain factor G'_δ and the overlap integral $M_\delta(z)$. The first term in (4) describes the Raman amplification of a seed light beam and the second one – Raman generation (Raman amplification of Stokes radiation, the source of which is spontaneous Raman scattering).

At the given $|F_p(z, \rho)|^2$, the determination of the overlap integral is reduced to finding the function $F(z, \rho)$ with the help of Eqn (1). However, even without addressing Eqn (1), we can draw some general conclusions about the possible values of this integral. In particular, it follows from expression (3) that in the plane-wave approximation $M_\delta(z) = 1$. The integral $M_\delta(z)$ is approximately equal to unity in those cases when the Stokes beam cross section is significantly smaller than the pump beam cross section. In all other cases, $M_\delta(z) < 1$. Here, $M_\delta(z)$ cannot be substantially smaller than unity for the Stokes beam cross section is formed by the pump and because of this cannot be larger than the pump beam cross section. The integral $M_\delta(z)$ is the part of the exponent which under conditions of a real experiment takes large values (more than 20). Thus, the weak dependence of $M_\delta(z)$ on δ can significantly affect the spectrum of the amplified Stokes beam. Consider this effect in the case of pumping by Gaussian and Bessel beams.

2.2 Pumping by a Gaussian beam

The Gaussian beam, as is known, is defined by the relations

$$|F_p(z, \rho)|^2 = \exp[-\alpha'_p(z)\rho^2], \quad S_p(z) = P_p \alpha'_p(z)/(\pi w_0^2), \quad (6)$$

where P_p is the pump beam power independent of z; $\alpha'_p(z) = 1/[1 + (z - z_0)^2/l_p^2]$ is the parameter determining the radius $w_p(z) = w_0/[\alpha'_p(z)]^{1/2}$ of the beam intensity distribution in the cross section z; z_0, $w_0 = w_p(z_0)$, $l_p = k_p w_0^2$ is the position, radius and the half the length of the beam waist; k_p is the wave number of pump radiation. Hereafter, the transverse coordinate ρ is normalised to the waist radius w_0.

In the case of the Gaussian pump, it is natural to model the scattered radiation field in the cross section z by the function

$$F(z, \rho) = \exp[-\alpha(z)\rho^2/2], \quad (7)$$

in which the complex parameter $\alpha = \alpha' + i\alpha''$ determines the radius $w_s = w_0\sqrt{\alpha'}$ of the intensity distribution and the radius $R = k_s w_0^2/\alpha''$ of the wave-front curvature of the scattered beam. It follows from physical assumptions that the use of function (7) for describing the Stokes beams is permissible when this beam is completely overlapped by the pump beam, i.e. when the condition $\alpha' > \alpha'_p$ is fulfilled. In situations when the Stokes beam develops from spontaneous scattered radiation, this conditions is fulfilled automatically.

As is shown in [9], α can be determined by using the equation

$$\frac{d\alpha}{dz} = -\frac{i}{kw_0^2}\alpha^2 + \frac{\gamma_\delta}{k_p w_0^2}\frac{\alpha_p'^2 \alpha'}{\alpha'_p + \alpha'} \quad (8)$$

obtained from (1), where $\gamma_\delta = \gamma'_\delta + i\gamma''_\delta = \gamma_0/(1 - i\delta)$. The parameter $\gamma_0 = k_p G_0 P_p/\pi$ means the plane-wave Raman gain at a distance equal to $l_p = k_p w_0^2$.

Analysis of equation (8) shows that when the condition $\alpha' > \alpha'_p$ is fulfilled, the quantity α is a slowly varying

function z and the derivative $d\alpha/dz$ can be neglected. As a result, we obtain the algebraic equation, whose solution has the from

$$\alpha(z) = \frac{1}{2}\left[1 + 2\left(|\gamma_\delta| + \gamma_\delta''\right)\frac{k}{k_p}\right]^{1/2}\left(1 - i\,\frac{\gamma_\delta'}{|\gamma_\delta| + \gamma_\delta''}\right)\alpha_p'(z). \quad (9)$$

It follows from (9) that the allowance for the imaginary part γ_δ'' of the Raman gain factor (i.e. the real part of the Raman susceptibility) leads to a decrease and to an increase in the radius $1/\sqrt{\alpha'}$ of the Stokes beam at $\gamma_\delta'' > 0$ (at $\delta > 0$) and $\gamma_\delta'' < 0$ (i.e. at $\delta < 0$), respectively, compared to the radius calculated at $\gamma_\delta'' = 0$. The phase front of this beam is convex in the direction of its propagation (a diverging beam), its curvature in the region $\delta > 0$ being smaller than that in the region $\delta < 0$. All this means that the real part of the Raman susceptibility produces a focusing and defocusing effect on high-frequency ($\delta > 0$) and low-frequency ($\delta < 0$) Stokes beam components, respectively.

The overlap integral $M_\delta(z)$ for the Stokes beam, described by function (7), is determined by the expression

$$M_\delta = \frac{\alpha_\delta'}{\alpha_p + \alpha_\delta'} = \left[\left(1 + 2\gamma_0\frac{k}{k_p}\varphi_\delta\right)^{1/2} - 1\right] \times \left[\left(1 + 2\gamma_0\frac{k}{k_p}\varphi_\delta\right)^{1/2} + 1\right]^{-1}, \quad (10)$$

where $\varphi_\delta = [(1+\delta^2)^{1/2} + \delta]/(1+\delta^2)$. Without taking into account the imaginary parts of the Raman gain factor (at $\gamma_\delta'' = 0$) the quantity M_δ is also determined by expression (10) but with the parameter $\gamma_\delta = 1/(1+\delta^2)$. The overlap integral in the case under study is independent of z. Taking into account this fact, expression (5) for the Raman gain assumes the form

$$D_\delta(z) = \gamma_\delta' M_\delta\left[\arctan\left(\frac{z - z_0}{l_p}\right) + \arctan\frac{z_0}{l_p}\right] \quad (11)$$

and the frequency dependence of the gain is determined by the function

$$g(\delta) = \frac{1}{1+\delta^2}\left[\left(1 + 2\gamma_0\frac{k}{k_p}\varphi_\delta\right)^{1/2} - 1\right] \times \left[\left(1 + 2\gamma_0\frac{k}{k_p}\varphi_\delta\right)^{1/2} + 1\right]^{-1}, \quad (12)$$

Figure 1 presents the dependences of $g(\delta)$ at different $\gamma_0 k/k_p$ calculated with and without the imaginary part of the Raman gain factor. One can see that the account for the imaginary part of G_δ increases and shifts the maximum of the function $g(\delta)$ to higher frequencies, this shift decreasing with increasing γ_0. By using expression (12) and the condition $dg(\delta)/d\delta = 0$, it is easy to show that the position of the maximum of the function $g(\delta)$ is determined by the relation

$$2\delta_m\left[\left(1 + 2\gamma_0\frac{k}{k_p}\varphi_\delta\right)^{1/2} + 1\right] = \left(1 + \delta_m^2\right)^{1/2}, \quad (13)$$

and its amplitude – by the relation

$$g_m = g(\delta_m) = \frac{\left(1 + \delta_m^2\right)^{1/2} - 4\delta_m}{\left(1 + \delta_m^2\right)^{3/2}}. \quad (14)$$

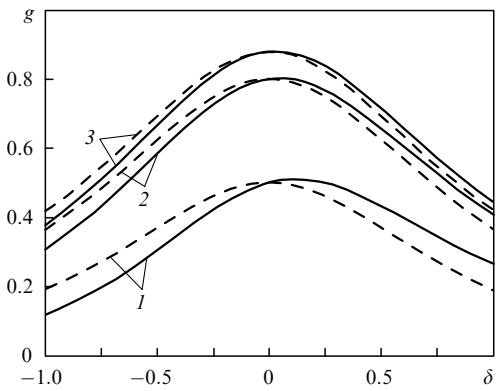

Figure 1. Functions of $g(\delta)$ at $\gamma_0 k/k_p = 4$ (*1*), 40 (*2*) and 120 (*3*) calculated taking into account (solid curves) and neglecting (dashed curves) the imaginary part of the Raman gain.

The quantities δ_m and g_m calculated with the help of expressions (13) and (14) as functions of the parameter $\gamma_0 k/k_p$ are shown in Fig. 2. For comparison the same figure presents the dependence $g(0)$ calculated with expression (12) and determining the amplitude of the maximum without taking into account the imaginary part of the Raman gain factor. Note that the difference $g_m - g(0)$ is always positive, i.e. the maximum of the Raman gain calculated by taking into account the imaginary part G_δ'' is always larger than the maximum of the Raman gain by neglecting G_δ''.

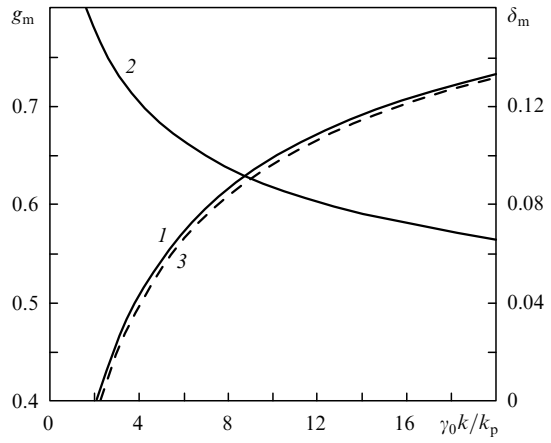

Figure 2. Amplitude g_m (*1*) and the position δ_m (*2*) of the maximum of function (12) and $g(0)$ (*3*) as functions of $\gamma_0 k/k_p$.

In the region of large γ_0 (virtually already at $\gamma_0 > 10$), δ_m and g_m can be determined by using the approximate expressions $\delta_m \approx 1/[2(2\gamma_0 k/k_p)^{1/2}]$ and $g_m \approx 1 - 2/(2\gamma_0 k \times k_p^{-1})^{1/2}$. Using expressions (4) and (11) it is easy to analyse the power spectrum of the amplified Stokes beam.

As was noted above, the second term in expression (4) describes Raman generation. Its source is spontaneous scattering. To estimate the power of this source, note that in the region z where the arctangent function can be replaced by its argument (for z, $z_0 < 0.3 l_p$), we have the relation

$$\int_0^z \exp[-D(z')]\,dz' = \frac{l_p}{\gamma_\delta' M_\delta}\left[1 - \exp\left(-\frac{\gamma_\delta' M_\delta z}{l_p}\right)\right].$$

If in this case the condition $\gamma_\delta M_\delta z/l_p \gg 1$ is fulfilled (for example, more than four) in the region $z < L$, the exponential in the derived relation can be neglected and expression (4) is reduced to the form

$$P_\delta(L) = [P_\delta(0) + \pi\eta w_0^2/M_\delta]\exp[D_\delta(L)], \quad (15)$$

where $D_\delta(L)$ is defined by expression (11).

Thus, the spectrum of the amplified radiation is determined by the spectrum of the gain $D_\delta(L)$, achieves the maximum at the maximal gain $D_{\delta m}$ and in the case $D_{\delta m} \gg 1$ has a Gaussian shape of width in $D_{\delta m}^{-1/2}$ times narrower than the spectrum of spontaneous scattering [6].

2.3 Pumping by a Bessel beam

Let pump radiation represent a Bessel beam obtained from a Gaussian beam with the help of an axicon. If the Gaussian beam waist is on the axicon, the Bessel beam field is determined by the relations

$$|F_p(z,\rho)|^2 = J_0^2(q_p\rho), \quad S_p(z) = \frac{P_p}{\pi w_0^2} f(z), \quad (16)$$

$$f(z) = 2\pi(n_p l_1 + z)\frac{q_p^2}{l_p}\exp\left[-(n_p l_1 + z)^2\left(\frac{q_p}{l_p}\right)^2\right], \quad (17)$$

where $J_0(q_p\rho)$ is the zero-order Bessel function; $q_p = k_p \times w_0\theta_p$; θ_p is the angle of inclination of the Bessel beam to the z axis in the scattering medium; l_1 is the distance between the axicon and the scattering medium; P_p and w_0 are the power and radius of the Gaussian beam at its entrance to the axicon; the coordinate z is measured from the input surface of the scattering medium. The field described by (16) exists in the region determined by the condition $0 < \rho < \rho_z$, where

$$\rho_z = \begin{cases} \theta_p(n_p l_1 + z)/w_0, & n_p l_1 + z < r_0/(2\theta_p), \\ r_0/w_0 - \theta_p(n_p l_1 + z)/w_0, & r_0/(2\theta_p) < n_p l_1 + z < r_0/\theta_p \end{cases}$$

is the Bessel beam radius in the cross section z; r_0 is the aperture radius on the axicon. If $r_0 > w_0$, it should be replaced in the presented inequalities by w_0. At points $z_m = w_0(\theta_p\sqrt{2})^{-1} - n_p l_1$, the function $f(z)$ has a maximum equal to $0.86\pi q_p$. At points $\rho_N = (\pi/q_p)(N + 3/4)$ at $N = 0, 1, 2, \ldots$, the function $|F_p(z,\rho)|^2$ is equal to zero. The parameter N determines the ring number of the Bessel beam and $\rho_0 = 3\pi/(4q_p)$ – the radius of its central spot to the base. The field $S_p(z)J_0^2(q_p\rho)$ has the maximum number of rings $N_m = q_p/\pi - 3/4$ in the cross section $z = w_0/(2\theta_p) - n_p l_1$.

It is known that the amplified Stokes radiation pumped by a Bessel beam consists of the conical and (or) axial components. Under the conditions when the depletion of the pump due to the Raman can be neglected, these components can be treated as independent modes. The transverse field structure of a conical mode can be described by the Bessel function: $F(z,\rho) = J_0(q\rho)$, where $q = kw_0\theta$ and θ is the angle of inclination of scattered radiation to the z axis. For this mode the overlap integral has the form

$$M_\delta(z) = \int_0^{\rho_z} J_0^2(q_p\rho)J_0^2(q\rho)\rho d\rho \Big/ \int_0^{\rho_z} J_0^2(q\rho)\rho d\rho. \quad (18)$$

Analysis shows [9] that expression (18), if considered as a function of the parameter q, has a maximum at the point $q = q_p$, and, hence, $\theta = (k_p/k)\theta_p$. Thus, the spectrum of the conical components according to relations (4) and (5) is completely determined by the frequency dependence of the Raman gain factor G'_δ, i.e. has a maximum at the point of the exact Raman resonance.

We will consider the spectrum of the axial mode of the Stokes beam in the case of the Bessel pump assuming that the mode field can be described by function (7). In this case, we obtain from (1) the equation [9]

$$\frac{d\alpha}{dz} = -\frac{i}{kw_0^2}\alpha^2 + \frac{\gamma_\delta}{k_p w_0^2} f(z)u(\alpha') \quad (19)$$

for determining the quantity α from (1), where

$$u(\alpha') = 2\alpha'^2\int_0^\infty [1 - J_0^2(q_p\rho)]\exp\left(-\alpha'\rho^2\right)\rho d\rho, \quad (20)$$

and expression (3) for the overlap integral assumes the form

$$M_\delta(z) = 2\alpha'\int_0^\infty J_0^2(q_p\rho)\exp\left(-\alpha'\rho^2\right)\rho d\rho. \quad (21)$$

Expressions (20) and (21) are written for the region z in which the radius ρ_z of the Bessel beam is significantly larger than the radius $1/\sqrt{\alpha'}$ of the Stokes beam.

In the region of large α' (at $\alpha' > q_p^2$ with the error less than 2 %) we can set $J_0^2(q_p\rho) \approx 1 - q_p^2\rho^2/4$ in expressions (20) and (21) and obtain correspondingly $u \approx q_p^2/4$, $M_\delta = 1 - q_p^2/(4\alpha')$,

$$\alpha' = [\varphi_\delta\gamma_0 q_p^2 f(z)k/(8k_p)]^{1/2}. \quad (22)$$

The condition of the applicability of this approximation is determined by the relation $\gamma_0 f(z) > 8q_p^2$ taking the form of a simple inequality $\gamma_0 > 3q_p$ in the region of the maximum of the function $f(z)$.

The expression for the Raman gain in this case assumed the form

$$D_\delta(\delta) = \gamma_0 g_b(\delta)\int_0^L f(z)dz, \quad (23)$$

where

$$g_b(\delta) = \frac{1}{1+\delta^2}\left[1 - \frac{b(1+\delta^2)^{1/2}}{(1+\delta^2)^{1/2} + \delta}\right] \quad (24)$$

is the function determining the gain spectrum. This spectrum is governed by one parameter $b = [2(k_p/k)/\gamma_0]^{1/2} \times T$, where $T = \int_0^L [q_p^2 f(z)/4]^{1/2}dz/\int_0^L f(z)dz$ is the parameter depending on the geometry of the experiment: the scattering medium thickness L, its distance l_1 from the axicon and radius ρ_0.

The dependence of the parameter b on the geometry of the experiment (parameters L, l_1 and ρ_0) differs significantly for the Bessel and Gaussian pumps; the latter at $\gamma_0 \gg 1$ is also described by expressions (22), (23), if every of the quantities $f(z)$ and $q_p^2/4$ in them is replaced by α'_p and if to take into account that after this replacement $T = 1$ and $b = [2(k_p/k)\gamma_0]^{1/2}$.

The possible values of the parameter T in the case of the Bessel pump, as a rule, significantly exceed a unity. For example, in the case, when the scattering medium is placed in the region of the maximum of the function $f(z)$ and its

thickness L is considerably smaller than the length of the Bessel beam waist w_0/θ_p (i.e. at $L \ll k_p w_0^2/q_p$) we have the relation $T = q_p[4f(z_m)]^{-1/2} = 0.54\sqrt{q_p}$. Under conditions of a real experiment we have $\sqrt{q_p} \sim 10 - 100$, and, hence, the parameter b in the case of the Bessel pump takes values which are ten times larger than in the case of the Gaussian pump of the same power (at the same γ_0).

The dependences of the position δ_m and the amplitude $g_b(\delta_m)$ of the maximum of function (24) on the parameter b are presented in Fig. 3. One can see that with increasing b, the shift δ_m of the maximum of the Raman gain rapidly increases. The amplitude of the maximum of the Raman gain proportional to $\gamma_0 g_b(\delta_m)$ grows linearly with $\sqrt{\gamma_0 q_p}$ in this case. Because at the fixed pump power the parameter b in the case of the Bessel pump is significantly higher than in the case of the Gaussian pump, one can easily conclude from Fig. 3 that the frequency shift of the axial component of the Stokes beam in the case of the Bessel pump should be considerably greater than that in the case of the Gaussian pump.

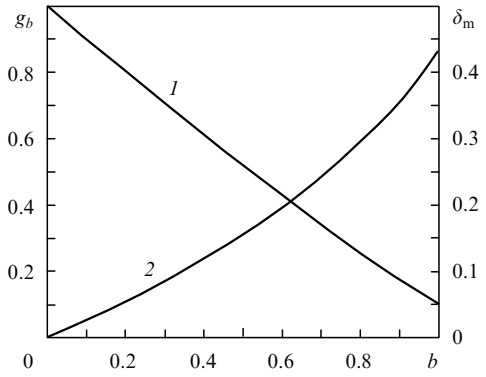

Figure 3. Dependences of the amplitude g_b (*1*) and the position δ_m (*2*) of the maximum of function (24) on the parameter b.

3. Experiment and discussion of the results

The frequency shift of the Raman gain upon pumping by Bessel and Gaussian beams was studied experimentally in the regime of Raman generation (amplification of the Stokes beam from the spontaneous noise level) in barium nitrate crystals. Crystals of length $L = 8$ cm were mounted at an angle to the pump beam axis to prevent the feedback. Their faces had an AR coating for the pump and Stokes radiation wavelengths. Scattering occurred at the vibrational frequency of 1047 cm^{-1}. The dephasing time of this vibration was $T_2 = 25$ ps [10], and hence the half-width of the spontaneous Raman scattering line was $\Delta\nu = 1/(2\pi T_2) =$ 6 GHz. Pumping was performed by using second harmonic radiation from a passively Q-switched 532-nm Nd : YAG laser. The laser generated a close-to-Gaussian beam ($M^2 = 1.1$) of radius $w_p = 1.6$ mm with the pulse energy of up to 5 mJ. The laser pulse duration FWHM τ_p was 10 ns, i.e. exceeded by several orders of magnitude the time T_2, which made it possible to consider the scattering process as quasi-steady-state. Measurements were performed near the Raman threshold (the conversion efficiency into Stokes radiation did not exceed 0.1 %).

3.1 SRS of a Bessel beam

The optical scheme of the experiment on studying the SRS pumped by a Bessel beam is presented in Fig. 4. Here the collimated Gaussian beam is transformed by the axicon into a quasi-Bessel beam with the angle at the cone vertex $\theta_p = 22$ mrad (in air). The barium nitrate crystal overlapped the central part of the Bessel beam. Stokes radiation at the crystal output was spectrally selected with the help of a glass filter. A part of radiation was directed to the CCD camera placed in the focal plane of lens L1 in order to detect its angular structure. The other part was analysed with the Fabry–Perot interferometer with a free spectral region of 15 GHz. The interference pattern was detected with the second CCD camera in the focal plane of lens L2.

Under the conditions described above, Stokes radiation was, as a rule, generated in the form of the conical and axial modes. Figures 5a, b show two realisations when either the conical or axial mode dominated. Quite frequently both modes with approximately equal intensities (Fig. 5c) were observed. The angular radius of the conical mode was $\theta \approx 23$ mrad, which in agreement with the condition of the transverse phase matching $\theta_p k_p = \theta k$. The divergence of the axial mode was three times lower. The Fabry–Perot interference patterns of the Stokes spectrum shown in Figs 5d–f represent a system of double rings. The doublet structure of the spectrum was observed in all detected realisations. If one of the generation channels (conical or axial) was blocked, one of the spectral components disappeared. This obviously indicates that the observed splitting of the spectrum is caused by the frequency differ-

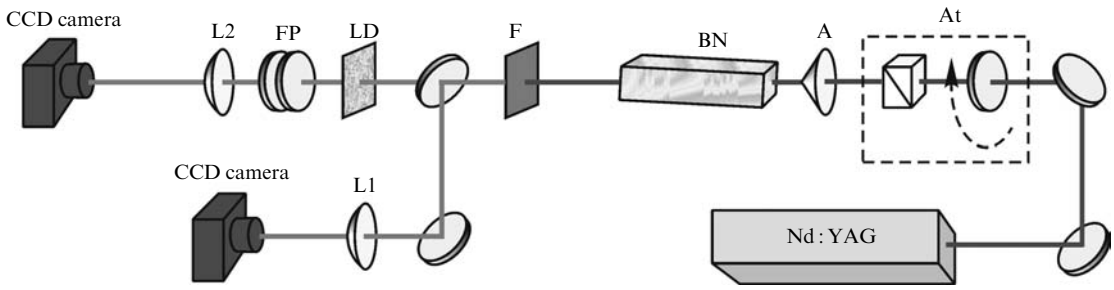

Figure 4. Optical scheme of the experiment on measuring the spectral shift between the axial and conical components of Stokes radiation in the case of the Bessel pump: (Nd : YAG) a single-mode single-frequency Nd : YAG laser (oscillation wavelength is 532 nm); (At) attenuator of laser pulse energy (half-wave plate and polariser for a wavelength of 532 nm); (A) glass axicon with the angle 3° at the base; (BN) 8-cm-long barium nitrate crystal; (F) glass filter; (LD) light diffuser; (FP) Fabry–Perot interferometer; (L1) lens with the focal distance $f_1 = 14$ cm; (L2) lens with the focal distance $f_2 = 50$ cm.

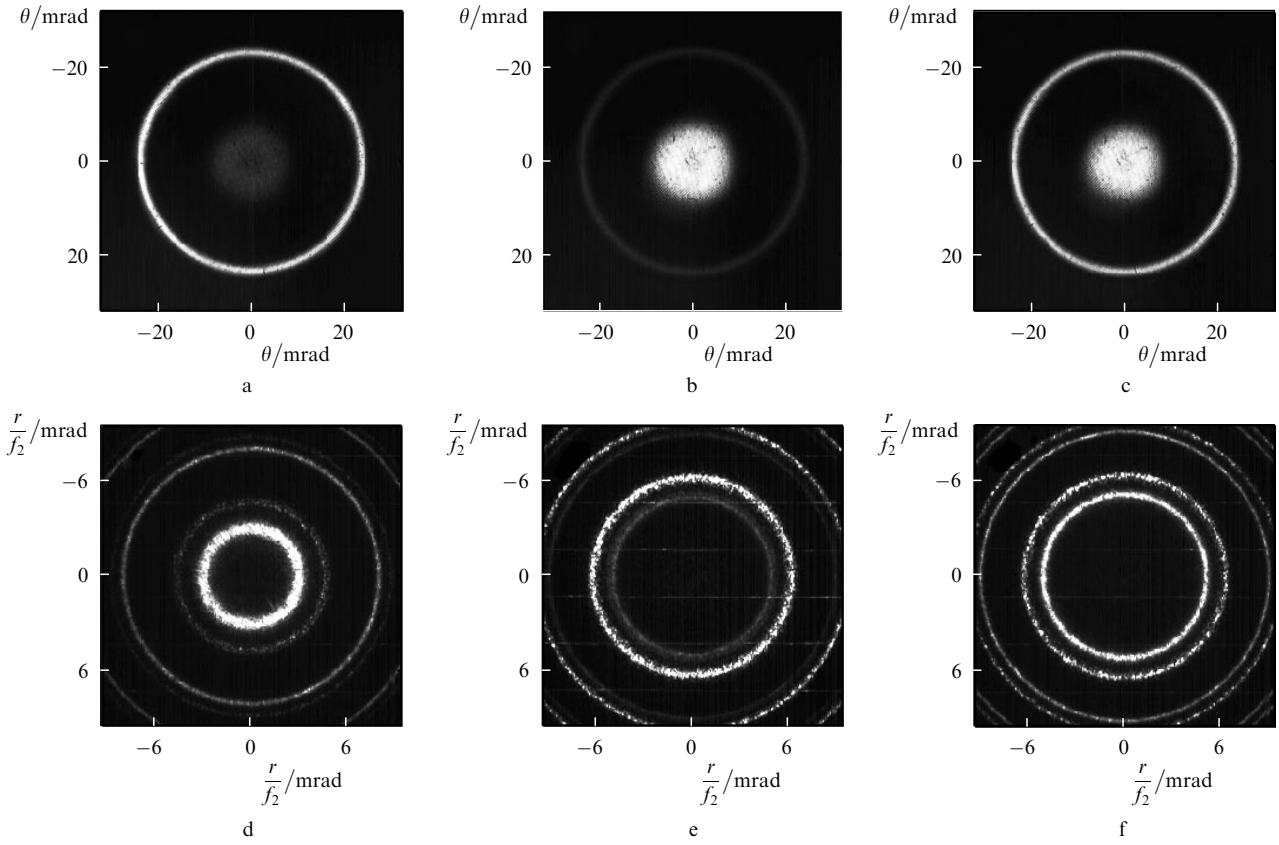

Figure 5. Examples of the far-field ransverse structure of Stokes radiation (a – c) and corresponding Fabry – Perot interference patterns (d – f) obtained in the experiment in the case of the Bessel pump.

ence in conical and axial modes. One can see from Fig. 5 that the generation frequency of the axial mode (external rings on the interference patters) is shifted to the high-frequency region with respect to the generation frequency of the conical mode (internal rings).

The presented interference patterns are the examples of the narrow-band generation at which the spectral bandwidths of generation of individual modes, approximately equal to 0.6 GHz, were smaller by more than an order of magnitude than the linewidth of the spontaneous Raman scattering. Some realisations had broader spectra (up to 2 GHz). Such fluctuations in the Stokes spectral are natural. In our experiment the average (with respect to the ensemble of realisations) width of the generation band of each mode was remarkably smaller than the linewidth of the spontaneous Raman linewidth and the frequency shift between the axial and conical modes significantly exceeded their spectral widths. The frequency shift measured over 50 realisations was 3.7 ± 0.6 GHz, which corresponds to 0.6 ± 0.1 of the Raman line HWHM of barium nitrate.

3.2 Comparison of shifts in the case of Gaussian and Bessel pumps

The optical scheme of the experiment aimed at comparing the frequency shifts of the Stokes radiation in the case of the Bessel and Gaussian pumps is presented in Fig. 6. In this experiment we used two generation channels. Initially, the identity between channels was established by pumping both of them by Gaussian beams. In this case, the single-mode laser beam was preliminary split into two. Then the beams were focused by lenses L3 and L4 with identical focal lengths to the centres of the crystals. The Stokes beams of different channels were combined with each other. Their spectral structure was analysed interferometrically with the help of a CCD camera placed in the focal plane of lens L2. To identify each channel in the interference pattern, a polarisation duplex was mounted in front of the camera, whose top and bottom half-planes had mutually orthogonal transmission axes [11]. In this case, a $\lambda/2$ plate was inserted into one of the generation channels, which rotated the polarisation plane of Stokes radiation of this channel by the angle $\sim 45^\circ$.

Then the optical scheme of the experiment was changed as follows. Lens L3 was replaced by the axicon which produced the Bessel beam with the angle at the cone vertex $\theta_p = 30$ mrad. This beam excited the SRS in the barium nitrate crystal, which was placed directly behind the axicon. The excitation conditions corresponded to generation of only the axial Stokes beam with the transverse intensity profile close to super-Gaussian and with the divergence $\theta \approx 10$ mrad. The generation channel with the Gaussian pump beam was used as a reference one.

Figure 7 presents typical interference patters obtained when pumping in both channels was performed by Gaussian beams. Figures 7a and b correspond to situations when one of two generation channels is blocked. The polarisation plane of Stokes radiation in the second generation channel is rotated by the angle 45° with respect to the transmission axes of the polarisation duplex. Figure 7c demonstrates radiation of both channels detected simultaneously. One can see from the interference patters that the positions of generation bands of Stokes radiation in different channels

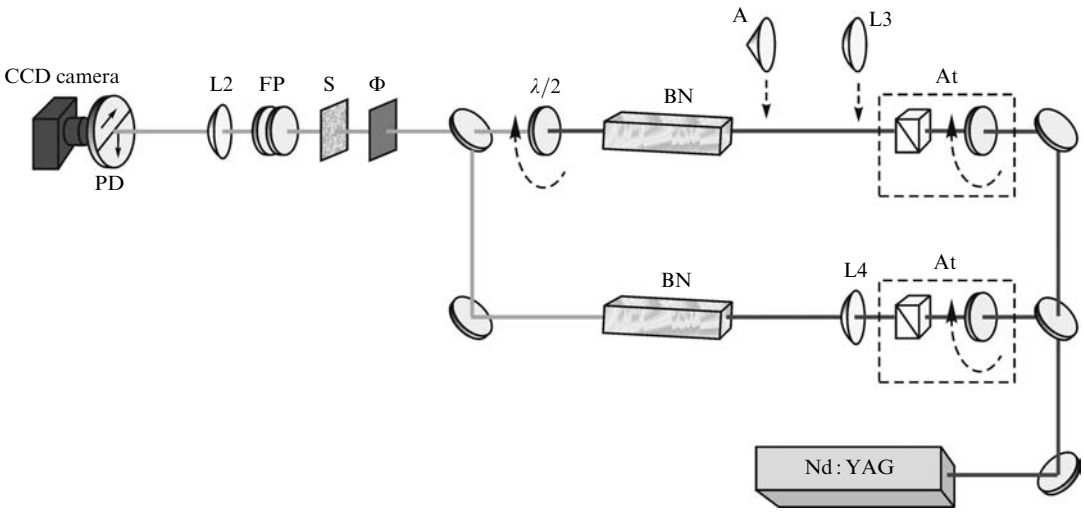

Figure 6. Optical scheme of the experiment on measuring the spectral shift between two generation channels of Stokes radiation: (L3, L4) lenses with the focal distance $f_3 = 30$ cm; (A) glass axicon with the angle 4° at the base; ($\lambda/2$) half-wave plate for a wavelength of 532 nm; (PD) polarisation duplex; other notations are the same as in Fig. 4.

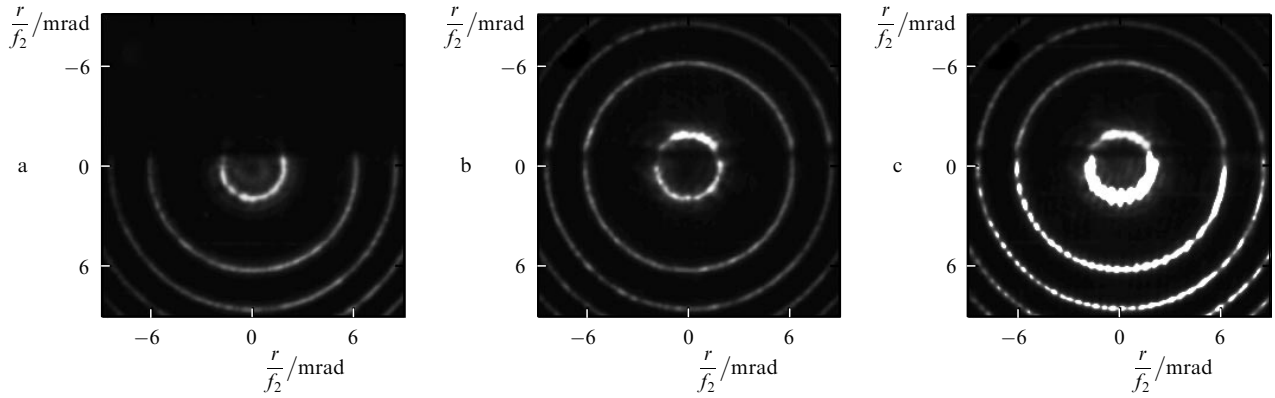

Figure 7. Examples of Fabry–Perot interference patterns of Stokes radiation obtained in the experiment upon pumping both generation channels by Gaussian beams in the case when one of the channels is open (a, b) and when both channels are open (c).

coincide. Analysis of 40 interference patterns showed that the shift of generation bands in different channels with respect to each other did not exceed 0.1 of the spontaneous Raman line HWHM.

Figure 8 presents the examples of interference patterns obtained with the Bessel pump beam used in one of the generation channels. The frequencies of the axial Stokes beam in the case of the Bessel pump (full rings) and Stokes generation in the case of the Gaussian pump are distinctly resolvable. Their difference measured in 30 realisations was 3.1 ± 0.8 GHz, i.e. 0.5 ± 0.1 of the Raman line HWHM in barium nitrate.

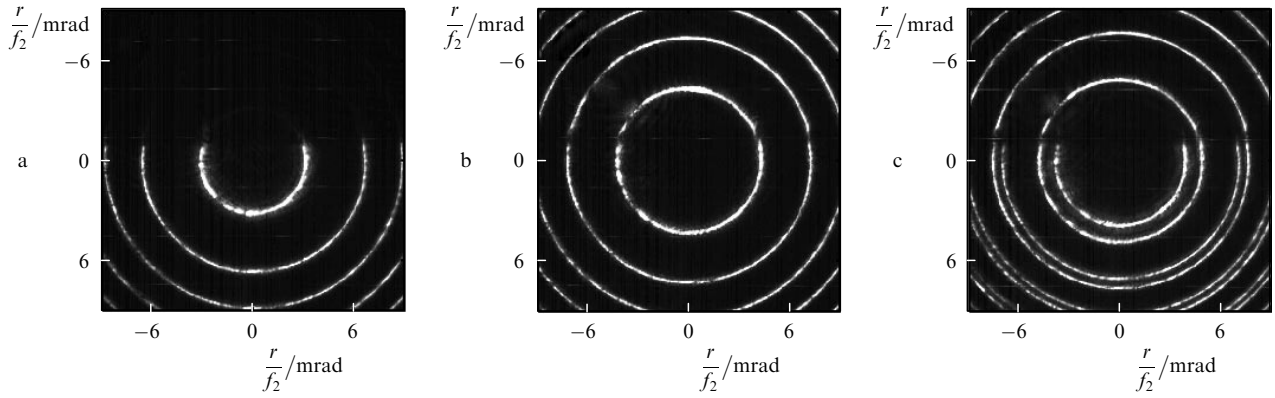

Figure 8. Examples of Fabry–Perot interference patterns of Stokes radiation demonstrating the frequency shift of amplified Stokes radiation in the case of the Bessel and Gaussian pumps: generation channels pumped by Gaussian (a) and Bessel (b) beams, both generation channels (c).

3.3 Discussion of the results

Thus, it follows from the experimental data that the axial and conical components of the Raman generation in the case of the Bessel pump have different frequencies, the frequency of the axial component being significantly shifted to the high-frequency region with respect to the conical component and that the frequency shift of the axial component in the case of the Bessel pump considerably exceeds the frequency shift of the Raman generation in the case of the Gaussian pump. This experimental result is in qualitative agreement with the conclusions of the theory presented above. Therefore, it is explained by the manifestation of the real part of the Raman susceptibility in the spectra of amplified radiation under conditions of the spatial inhomogeneity of the pump, i.e. under the conditions when the pump-induced focusing of high-frequency components of the Stokes beam resulting from the contribution of the real part of the Raman susceptibility to the refractive index of the medium, leads to the increase in the overlap integral of interacting beams and in the efficiency of the Raman amplification.

Unfortunately, the quantitative comparison of the results of the theory developed in this paper and the experiment performed are cumbersome. In theoretical relations the frequency dependence of the Raman gain is governed by the parameter $\gamma_0 = k_p G_0 P_p/\pi$ proportional to

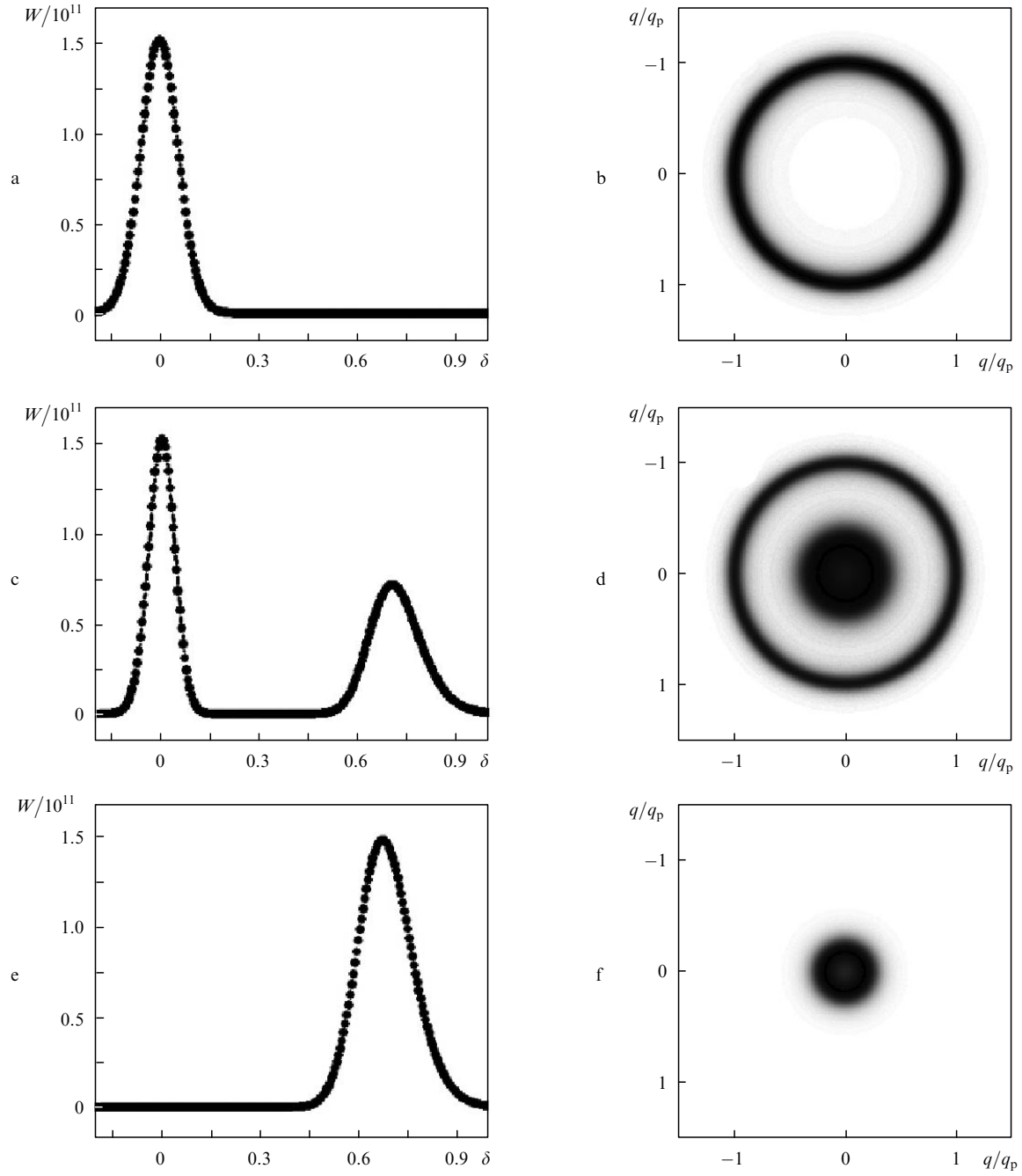

Figure 9. Spectra (a, c, e) and far-field structures of amplified Stokes radiation (b, d, f) calculated for the Bessel pump beams with $q_p = 414$, $\gamma_0 = 200$ (a–d) and $q_p = 566$, $\gamma_0 = 200$ (e, f) taking into account (a, b) and neglecting (c–f) the imaginary part of the Raman gain factor (at $G''_\delta = 0$).

the pump beam power P_p and in the case of the Bessel pump – also by the parameter $q_p = k_p\theta_p w_0$. In the experiment $\gamma_0 \approx 200$, and $q_p = 414$ (at $\theta_p = 22$ mrad) and 566 (at $\theta_p = 30$ mrad). For these γ_0, the frequency shift δ_m in the case of the Gaussian pump should be significantly lower than 0.1. At the same time the measurement error in δ_m was ~ 0.1. As was noted above, the developed theory for the case of the Bessel pump is applicable under the condition $\gamma_0 > 3q_p$. In the experiment this condition was hardly fulfilled.

At $\gamma_0 < q_p$, we failed to construct the analytic solution of equation (1). Therefore, to increase the reliability of the results obtained, we analysed the δ dependence of the quantity

$$W(\delta) = \int |E(L,\rho)|^2 \rho \mathrm{d}\rho \Big/ \int |E(0,\rho)|^2 \rho \mathrm{d}\rho,$$

having the sense of the Raman amplification efficiency of the seed field $E(0,\rho)$ in the medium of thickness L. This was done by solving numerically equation (1) for the Bessel pump beam, which was determined by expressions (16) and (17). Other parameters were close to those realised in the experiment. The intensity of Stokes radiation at the input to the scattering medium $|E(0,\rho)|^2$ was given in this case by the function $\exp(-\rho^2/\rho_0^2)$ with the radius of the transverse structure equal to the radius ρ_0 of the central core of the Bessel beam. Figure 9 presents the results of this analysis. Figure 9a and c show the dependences of $W(\delta)$ calculated with and without the allowance for the imaginary part G''_δ of the Raman gain factor, and Figs 9b and d – angular structures of amplified beams corresponding to them (their fields in the far-field region). One can see that the frequency of the conical component coincides with the frequency of the exact Raman resonance, while the frequency of the axial component is considerably shifted to the high-frequency region with respect to it. Figures 9e and f illustrate the situation when only the axial component is manifested in the Raman amplification.

4. Conclusions

In this paper we present the results of the theoretical and experimental investigation on the manifestation of the real part of the Raman susceptibility in the spectra of Stokes radiation amplified from the level of the spontaneous Raman scattering (Raman generation) upon irradiation of the scattering medium by the Gaussian or Bessel pump beams. Relations have been obtained which allow comparatively simple estimation of the Raman amplification efficiency and spectral characteristics of the Stokes beam in different cases. It is shown that the account for the real part of the Raman susceptibility leads to an increase in the overlap integral of the Stokes beam and the pump beam and, as a result, to the increase in the efficiency of the Raman generation in the range of frequencies higher than the frequency corresponding to the maximum of the spontaneous Raman scattering. Due to this, there occur high-frequency shifts of the Stokes spectrum in the case of the Gaussian pump and of the axial component of the Raman generation in the case of the Bessel pump. In the latter case the shift is significantly higher, which is demonstrated in the experiments on the Raman generation in barium nitrate crystals. The conical components appearing in the case of the Bessel pump is generated at the frequency corresponding to the maximum of the spontaneous Raman scattering.

Acknowledgements. The authors thank V.E. Agabekov for placing at our disposal the materials for fabricating a polarisation duplex.

References

1. Akhmanov A.S., Khokhlov R.V. *Problems of Nonlinear Optics* (New York: Gordon and Beach, 1972; Moscow: Izd. VINITI, 1964).
2. Bloembergen N. *Nonlinear Optics* (New York: W.A. Benjamin Inc., 1965; Moscow: Mir, 1966).
3. Owyoung A. *Appl. Phys. Lett.*, **26**, 168 (1975).
4. Cotter D., Hanna D.C., Wyatt R. *Appl. Phys.*, **8**, 333 (1975).
5. Repasky K.S., Carlsten J.L. *Phys. Rev. A*, **54**, 4528 (1996).
6. Apanasevich P.A., Timofeeva V.A. *Zh. Prikl. Spektros.*, **74**, 230 (2007).
7. Apanasevich P.A., Chulkov R.V., Timofeeva V.A. *Zh. Prikl. Spektros.*, **75**, 336 (2008).
8. Chulkov R., Grabtchikov A., Apanasevich P., Orlovich V. *Opt. Lett.*, **33**, 2728 (2008).
9. Apanasevich P.A., Chulkov R.V., Timofeeva V.A. *Zh. Prikl. Spektros.*, **71**, 778 (2005).
10. Zverev P.G., Basiev T.T., Osiko V.V., Kulkov A.M., Voitsekhovskii V.N., Yakobson V.E. *Opt. Mater.*, **11**, 315 (1999).
11. Kyzylasov Yu.I., Starunov V.S., Fabelinskii I.L. *Pis'ma Zh. Eksp. Teor. Fiz.*, **11**, 110 (1970).